



Molecular Crystals and Liquid Crystals

Publication details, including instructions for authors and subscription information:

<http://www.tandfonline.com/loi/gmcl20>

Luminescence in Anodic ZrO_2 Doped with Eu(III) ions

F. Trivinho-Strixino^a, F. E. G. Guimarães^b & E. C. Pereira^a

^a NANOFAEL, LIEC, Universidade Federal de São Carlos, São Carlos, SP, Brazil

^b Universidade Estadual de São Paulo, Instituto de Física de São Carlos, Grupo de Semicondutores, São Carlos, SP, Brazil

Version of record first published: 31 Aug 2012.

To cite this article: F. Trivinho-Strixino, F. E. G. Guimarães & E. C. Pereira (2008): Luminescence in Anodic ZrO_2 Doped with Eu(III) ions, *Molecular Crystals and Liquid Crystals*, 485:1, 766-775

To link to this article: <http://dx.doi.org/10.1080/15421400801913444>

PLEASE SCROLL DOWN FOR ARTICLE

Full terms and conditions of use: <http://www.tandfonline.com/page/terms-and-conditions>

This article may be used for research, teaching, and private study purposes. Any substantial or systematic reproduction, redistribution, reselling, loan, sub-licensing, systematic supply, or distribution in any form to anyone is expressly forbidden.

The publisher does not give any warranty express or implied or make any representation that the contents will be complete or accurate or up to date. The accuracy of any instructions, formulae, and drug doses should be independently verified with primary sources. The publisher shall not be liable

for any loss, actions, claims, proceedings, demand, or costs or damages whatsoever or howsoever caused arising directly or indirectly in connection with or arising out of the use of this material.

Luminescence in Anodic ZrO₂ Doped with Eu(III) ions

F. Trivinho-Strixino¹, F. E. G. Guimarães²,
and E. C. Pereira¹

¹NANOFAEL, LIEC, Universidade Federal de São Carlos, São Carlos, SP, Brazil

²Universidade Estadual de São Paulo, Instituto de Física de São Carlos, Grupo de Semicondutores, São Carlos, SP, Brazil

Photoluminescence and structure properties of anodically prepared ZrO₂ oxide films doped with Europium (III) ions were investigated. Microstructural analysis reveals that the predominant crystallographic structure is the monoclinic phase with small quantities of tetragonal and cubic phases. Important crystallite size and isotropic strain are observed for the monoclinic phase and they are related to the incorporation of Europium (III) ions inside the oxide matrix. The photoluminescence spectrum reveals a broad emission band in the range between 350–650 nm related to the ZrO₂. Emission lines corresponding to transitions from the lowest emitting ⁵D₀ level of Eu(III) to several sublevels of the ground state level ⁷F_{0, 1, 2, 3, 4 were also observed.}

Keywords: anodic doping; anodic zirconium oxide; europium; photoluminescence; rare-earth

INTRODUCTION

Zirconium oxide is known to have excellent technological properties such as chemical and thermal stability, mechanical strength and wear resistance as well as its good ion-exchange properties [1,2]. Due to the high oxygen conductivity of the cubic ZrO₂, it has been applied in high temperature solid oxide fuel cells and as industrial catalyst oxygen sensors [3,4]. This material is also present on the surface of nuclear fuel rods [1,5]. Besides its well known ceramic properties, mentioned

The authors are grateful to FAPESP and CNPq for the financial support.

Address correspondence to Ernesto Pereira, NANOFAEL, LIEC, Universidade Federal de São Carlos (DQ-UFSCar), Cx.P.: 676, São Carlos, SP, 13565-905, Brazil.
E-mail: deep@power.ufscar.br

before, ZrO₂ has also a very small stretching frequency (470 cm⁻¹) when compared to other host materials [6]. This low phonon energy opens up the possibility of higher efficient luminescence of active ions incorporated into ZrO₂ matrix [7].

A considerable amount of papers has been reported on the mechanical and other physical properties of ZrO₂, whereas only little research work has been done on the luminescence properties of this material [1,2,7,8]. Considering all above, zirconium oxide is a material that deserves attention in the field of photonics. It can be used in a variety of photonics and industrial applications [1,2,7,9,10]. In special, the interest on this rare earth doped phosphor is to produce visible emission for application such as solid state lighting, displays and new-generation television screens [7].

In this work, we present a method to obtain doped ZrO₂ named anodic doping [11], using an electrochemical technique. The advantages of this method are the low cost and the possibility to dope the material with different ions with high doping levels. The preparation parameters (temperature, concentration and current density) should be set in a proper manner in order to enable the anodic doping of specific ions. We have already described this method for Ca doped ZrO₂, where a modification in the microstructure of the oxide was observed [11].

MATERIALS AND METHODS

Annealed Zirconium (Zr) foils (Alfa Aesar 99,8%, 0.25 mm thick) were cut in flag format. These foils were anodized in aqueous electrolyte solution containing 0.1 M H₃PO₄ to obtain pure ZrO₂ as reference. Europium (III) doped ZrO₂ was produced in aqueous electrolyte solution containing 0.04 M H₃PO₄, 0.05 M C₆H₈O₇ (citric acid) and 5.3×10^{-4} M EuCl₃. Two Pt sheets were used as counter electrodes to obtain a homogeneous electric field distribution over the electrode surfaces. A homemade DC power supply was used to perform the experiments. All Zr foils were anodized under a constant current density of 16 mA/cm². The electrolytic cell was maintained in a constant temperature at 20°C. The electrolyte was stirred using a magnetic stirrer. Prior to anodization, the Zr flags were mechanically polished and washed in boiling water with Extran[®] solution. The voltage x charge curves were recorded using a HP-Agilent model 3440 A Digital Multimeter coupled to a computer.

The structural analysis was carried out using an XRD RIGAKU[®] with CuK_α radiation ($\lambda = 1.54056 \text{ \AA}$) with 40 KV and 150 mA applied in the anode. The microstructural analysis was performed using the GSAS-EXPGUI refinement program and the Le Bail method.

The samples were excited using a He–Cd (KIMON[®]) LASER with $\lambda = 325$ nm and the emission spectra were collected using a SPEX[®] MD500 spectrometer in perpendicular direction. A band pass filter (cut-off at 345 nm) was used in front of the spectrometer window to avoid back scattered laser light.

UV-Vis absorbance was carried out using a spectrophotometer Cary 5 G (Varian[®]) with the diffuse reflectance accessory. Kubelka-Munk transformation was performed to correct the spectral data for high scattering samples and to evaluate the absorbance characteristics.

RESULTS

Anodization Curves

Figure 1 depicts the voltage-charge curve during constant current anodization of zirconium. The anodic oxide formation under galvanostatic regime is characterized by two regions [12]: the initial one presents an almost linear increase of the voltage with time up to 450 V. This region is characterized by the increase of thickness of the barrier type oxide. Since the voltage is a linear function of the

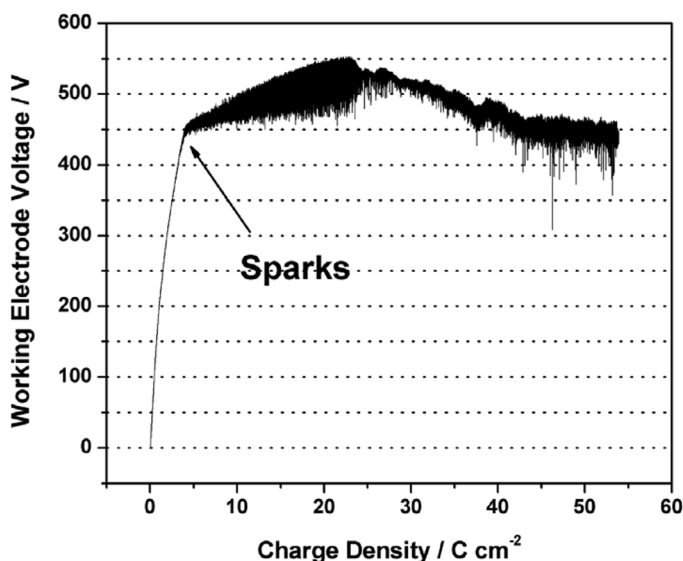


FIGURE 1 Voltage-Charge curve for Eu(III)-doped ZrO₂ anodization in 0.04 M H₃PO₄ + 0.05 M Citric Acid + 5.3×10^{-4} M EuCl₃ aqueous solution, $i = 16 \text{ mAcm}^{-2}$, $T = 20^\circ\text{C}$.

thickness at constant current density and constant molar volume, this region could be associated with the film growth controlled by the ionic transport [11]. The second region is characterized by voltage oscillation with amplitudes ranging from 20 V up to 80 V for charge values between 5 and 55 C cm^{-2} . The beginning of the voltage oscillation indicates that a dielectric breakdown occurs, which could be explained in terms of localized breakdown events in the film [13]. Both dissolution and electronic transport become important in this voltage range. Intense generation of sparks was observed in the film during anodization after 5 C cm^{-2} .

XRD Microstructure Characterization

The X-ray diffraction patterns (XRD) for pure ZrO_2 and Eu(III)-doped ZrO_2 formed anodically are illustrated in Figure 2. Zirconium oxide can occur in three different phases [14,15]. At low temperatures, a

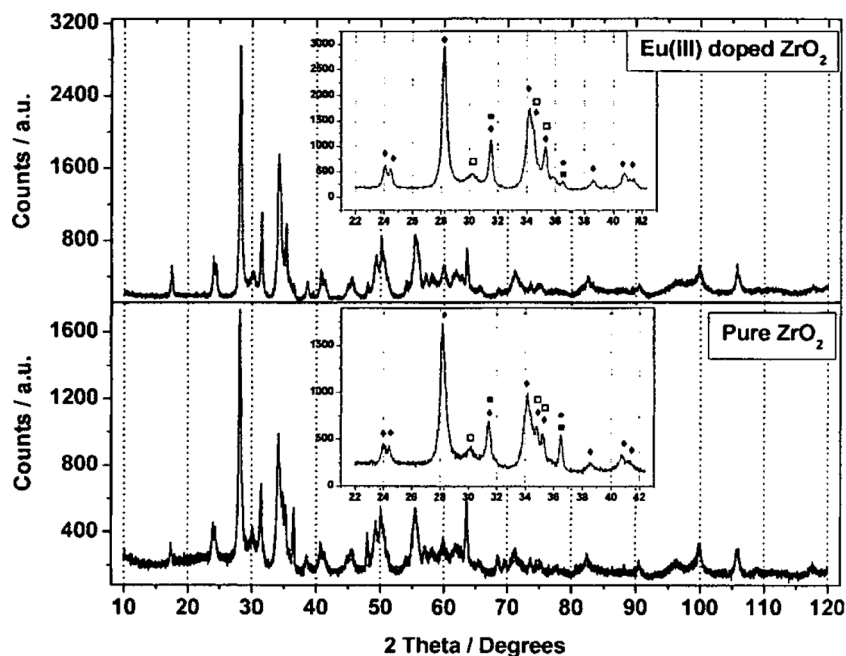


FIGURE 2 X-ray diffractograms for the pure anodically prepared ZrO_2 film and Eu(III)-doped ZrO_2 film. Insets: detailed area from XRD spectrum. (♦) Monoclinic phase, (□) Tetragonal phase, (■) Cubic phase and (●) Hexagonal phase (metallic Zr).

monoclinic phase is formed, which is converted into a tetragonal phase at 1200°C and finally into a cubic phase at 2370°C. The main XRD peaks for the monoclinic phase occur at $2\theta = 28.15^\circ$ and 34.16° [10,11]. The tetragonal and cubic phases are assigned mainly by XRD peaks, at $2\theta = 30.14^\circ$ and $2\theta = 31.45^\circ$, respectively [10,11]. Therefore, Figure 2 shows that the monoclinic phase is predominant, although the other ones can be detected in small amounts. Since the metal diffraction peaks (hexagonal phase) are also observed at $2\theta = 36.48^\circ$, we assume that the oxide film thickness is thin enough to expose the metal diffraction.

Table 1 summarizes the results from X-ray analysis performed using the Le Bail Method [16,17]. It is important to emphasize that the estimation of the phases composition could not be performed since the anodically prepared zirconium oxide is attached to the zirconium metallic substrate. Hence, a Rietveld analysis [17] would imply significant errors from composition quantities. To avoid this, the Le Bail Method refinement, included on the EXPGUI refinement package [16], was used to analyze the XRD patterns and to evaluate the profile parameters, namely crystallite size, isotropic strain and cell parameters. The results obtained show an important variation of the crystallite size and the isotropic strain for the monoclinic phase, comparing pure and doped ZrO_2 . This variation can be related to a microstructure deformation due to the incorporation of Eu(III) inside the oxide matrix.

Optical Characterization

Figure 3 shows the photoluminescence (PL) of the pure and Eu(III) doped ZrO_2 . A broad emission band is seen in the range between

TABLE 1 Lattice Parameters, Crystallite Size and Isotropic Strain for Pure ZrO_2 and Eu(III) Doped ZrO_2

Film	Crystallographic phase	Cell parameters (Å)				Crystallite size (nm)	Isotropic strain (%)
		a_0	b_0	c_0	β		
ZrO_2	Monoclinic	5.155	5.200	5.313	99.03	29.3	0.57
	Tetragonal	3.597	3.597	5.197		11.0	0.78
	Cubic	4.922	4.922	4.922		134.8	0.40
Eu(III) doped ZrO_2	Monoclinic	5.156	5.204	5.316	99.08	45.4	0.96
	Tetragonal	3.601	3.601	5.194		10.9	0.62
	Cubic	4.923	4.923	4.923		142.5	0.55

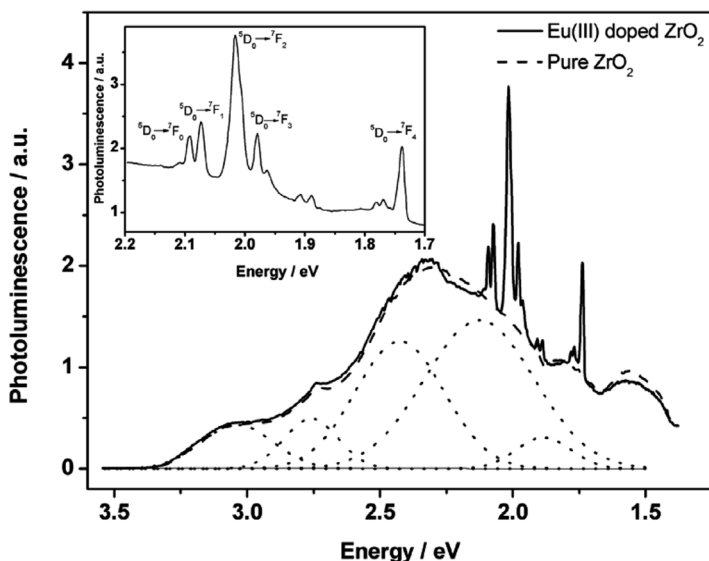


FIGURE 3 Emission spectra of Eu(III)-doped ZrO₂ prepared in 0.04 M H₃PO₄ + 0.05 M Citric Acid + 5.3×10^{-4} M EuCl₃ aqueous solution, $i = 16 \text{ mA cm}^{-2}$, $T = 20^\circ\text{C}$. Laser $\lambda_{\text{exc}} = 325 \text{ nm}$ (3.8 eV) and $T = 4.7 \text{ K}$. Inset: E(III) emission lines in detail.

350 nm (3.54 eV) and 740 nm (1.68 eV) with two shoulders centered at 3.05 eV and 2.74 eV, and a maximum at 2.33 eV. These bands are related to the oxide matrix emission probably originated from defects and impurities introduced during the film formation [1,3,6,12,18,19]. The luminescence spectrum of the ZrO₂ doped sample exhibits additional emission lines corresponding to transitions from the lowest emitting $^5\text{D}_0$ level of Eu(III) to several sublevels of the ground state level $^7\text{F}_0$, 1, 2, 3, 4 ($e_{\text{max}} = 2.09, 2.07, 2.02, 1.98$ and 1.74 eV , respectively) [20], among which the emission line with $e_{\text{max}} = 2.02 \text{ eV}$ ($^5\text{D}_0 \rightarrow ^7\text{F}_2$ transition) is the most intense. In addition, Figure 3 shows that the Eu(III) emission lines are asymmetric, which could be related to the fact that these ions behave as point defect in the ZrO₂ host matrix (insets in Fig. 3). The DRX analysis corroborates this proposition (Fig. 2 and Table 1). Since the absorption cross section for Eu is small for the laser excitation light at 325 nm (3.8 eV), we expect that the intense Eu emissions are a consequence of electronic energy transfer from the ZrO₂ host states, which are superposed to the electronic states of Eu(III) ions in the energy range below 3.8 eV (Fig. 4).

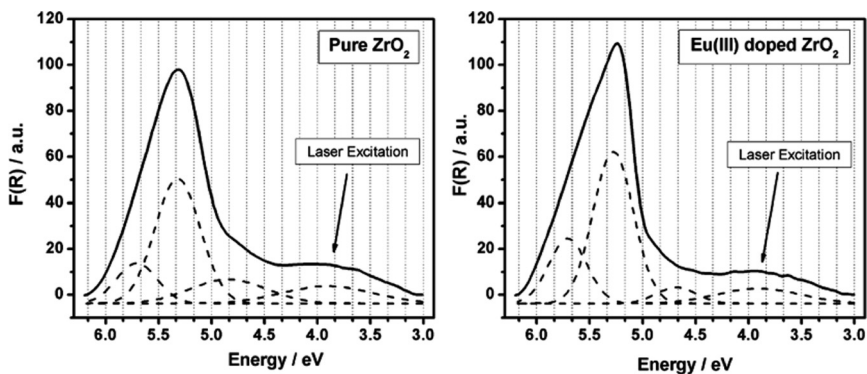


FIGURE 4 Kubelka-Munk corrected spectra for pure and Eu(III)-doped ZrO_2 prepared in 0.04 M H_3PO_4 + 0.05 M Citric Acid + 5.3×10^{-4} M EuCl_3 aqueous. $i = 16 \text{ mA cm}^{-2}$, $T = 20^\circ\text{C}$. Arrows indicate the Laser excitation energy during PL measurements.

The absorbance response and the respective deconvoluted parameters can be observed in Figure 4 and Table 2. It can be seen that the Kubelka-Munk corrected absorbance spectra have almost the same shape for pure and Eu(III)-doped zirconium oxide. From this figure, one can observe an intense broad absorption band centered at 5.7 eV, which is the band gap of ZrO_2 [3]. Along this broadband, one can also observe a small broadband at ~ 4 eV, present in both films, pure and doped ZrO_2 . From the results presented in Figure 4,

TABLE 2 Spectroscopic Parameters Extracted from Deconvolution of Absorbance Spectra (Fig. 4) of ZrO_2 and Eu(III)-doped ZrO_2

Films	Peak	Center (eV)	FWMV (eV)	Normalized integrated area	Normalized amplitude
Fit accuracy (r^2) = 0.9987					
Pure ZrO_2	Peak 1	3.9	1.014	0.276	0.140
	Peak 2	4.8	0.849	0.327	0.194
	Peak 3	5.3	0.503	1	1
	Peak 4	5.7	0.453	0.291	0.325
Fit accuracy (r^2) = 0.9948					
Eu(III)-doped ZrO_2	Peak 1	3.9	0.929	0.204	0.099
	Peak 2	4.7	0.447	0.106	0.107
	Peak 3	5.3	0.449	1	1
	Peak 4	5.7	0.423	0.404	0.429

one can estimate the excited electronic states of the pure and Eu(III)-doped ZrO₂ and correlate them with the emission electronic states observed in Figure 3. The origin of these bands can be related to the existence of oxide defects and emission recombination center lying in the band gap region of the ZrO₂ host.

DISCUSSIONS

From the microstructure data (Fig. 2 and Table 1), one can observe that the diffraction lines from Eu₂O₃ are not present. This oxide could be formed due to the intense applied electrical field (in the order of 10⁶ V/m). Instead, an increase in the crystallinity of the Eu(III)-doped ZrO₂ in comparison with pure ZrO₂ was observed. This result can be better visualized in Table I, which depicts some crystallographic parameters calculated from the Le Bail refinement procedure. The only important modification in the microstructure parameters is observed at the monoclinic phase (predominant phase for both films). The crystallite size for the Eu doped ZrO₂ monoclinic phase increased almost 65% (Table I). One possible explanation for this fact could be the incorporation of Eu(III) ions in the oxide host matrix, which causes a deformation of the Zr and O atoms bonds and angles. The isotropic strain could be a diagnosis of this behavior. From this parameter, one can observe an increase of the isotropic strain of the monoclinic phase of almost 59% in comparison with the pure ZrO₂ (Table 1).

The photoluminescence observed for pure zirconium oxide could be explained in terms of the anodization theories [12,13,21] and the experimental conditions herein used. In general, the breakdown process after the barrier type film formation (after 5 C cm⁻² – Fig. 1) is always present. However, during the breakdown process, the oxide dissolution rate is too slow as compared to the oxide formation rate. Hence, the overall reactions occurring at the electrode are the water decomposition and the migration process of ions through the metal-oxide/oxide-electrolyte interface due to the high electric field (major ionic transport). Depending on the metal, there should be various combinations of mobile ionic species. Some authors [12,22,23] determined that the cationic transport number (t^+) for zirconium anodization is almost ≤ 0.05 . This means that the main transport process is solely due to anionic migration (O⁻, OH⁻, metal vacancies, electrolyte anions) inward the oxide towards the metal/oxide interface. However, Parkhutik [12] showed that even in oxides with only one type of moving ion, the increase of the current density above 10 mA/cm² may cause the movement of usually immobile species, especially for zirconium anodization. In this case, fields up to 5×10^8 V/m may cause

a flow of zirconium ions almost equal to that of oxygen ions through the film. Consequently, oxygen and metal vacancies (ionic defects) could be generated and might migrate in the corresponding direction due to the electric field. In our experiment, the large applied electric field causes cations and anions species to flow in opposite directions and some defects may be formed in the oxide structure. As a consequence, an expressive number of different kinds of structure defects may be produced in the oxide. For thermally prepared ZrO_2 [1,3,5,18,19], some authors described that the origin of the photoluminescence property could be related to these defects (for example, a single ionized oxygen vacancy, in the case of ZrO_2). Considering the exposed above, these models could explain our data, since the spectral shape and the emission energies are almost the same.

The incorporation of Eu(III) ions occurs during the dielectric breakdown phenomena since both local destruction and reconstruction of the oxide film take place during the anodization. During this local oxide destruction, a "hole" is created and filled with the solution containing the doping ions. Because of the high velocity of this destruction and reconstruction process, part of the ions are trapped inside the oxide, leading to the Eu(III) anodic doping. This kind of phenomenon was also observed for different anodic oxides and doping ions [11,24,25].

CONCLUSIONS

We described the synthesis of an anodically prepared ZrO_2 doped with Eu(III) ions using an electrochemical technique, named anodic doping. From the microstructural analysis, an important variation of the monoclinic crystallite size and isotropic strain was observed, which could be related to the incorporation of Eu(III) ions in the oxide host matrix. An intense PL broadband was observed in the range between 3.54 eV and 1.68 eV and it was assigned to the ZrO_2 host matrix. The characteristic emission lines of the Eu(III) ions were also observed. The incorporation of the doping ions was explained in terms of the dielectric breakdown mechanism of destruction and reconstruction of the anodic oxide films during anodization. During this process, electrolyte solution containing the doping ions can be trapped in the oxide host matrix.

REFERENCES

- [1] Yueh, H. K. & Cox, B. (2003). *J. Nucl. Mater.*, 323, 57.
- [2] Chen, H. R., Shi, J. L., Yang, Y., Li, Y. S., Yan, D. S., & Shi, C. S. (2002). *Appl. Phys. Lett.*, 81, 2761.

- [3] Emeline, A., Kataeva, G. V., Litke, A. S., Rudakova, A. V., Ryabchuk, V. K., & Serpone, N. (1998). *Langmuir*, 14, 5011.
- [4] Li, J., Bai, X. D., Zhang, D. L., & Li, H. Y. (2006). *Appl. Surf. Sci.*, 252, 7436.
- [5] Yueh, H. K. & Cox, B. (2004). *J. Nucl. Mater.*, 324, 203.
- [6] Reisfeld, R., Zelnor, M., & Patra, A. (2000). *J. Alloys Compd.*, 300, 147.
- [7] De la Rosa, E., Diaz-Torres, L. A., Salas, P., & Rodriguez, R. A. (2005). *Opt. Mater.*, 27, 1320.
- [8] Reisfeld, R., Saraidarov, T., Pietraszkiewicz, M., & Lis, S. (2001). *Chem. Phys. Lett.*, 349, 266.
- [9] Huong, T. T., Anh, T. K., Nam, M. H., Barthou, C., Strek, W., & Minh, L. Q. (2007). *J. Lumin.*, 122, 911.
- [10] Salas, P., De la Rosa-Cruz, E., Diaz-Torres, L. A., Castano, V. M., Melendrez, R., & Barboza-Flores, M. (2003). *Radiat. Meas.*, 37, 187.
- [11] Bensadon, E. O., Nascente, P. A. P., Olivi, P., Bulhoes, L. O. S., & Pereira, E. C. (1999). *Chem. Mater.*, 11, 277.
- [12] Parkhutik, V. P. et al. (1992). In: *Electric Breakdown in Anodic Oxide Films*, Conway, B., White, J., & Bockris, J. O. M. (Eds.), Plenum Press: New York, 391.
- [13] Ikonopisov, S. (1977). *Electrochim. Acta*, 22, 1077.
- [14] Montero, I., Albella, J. M., & Martinezduart, J. M. (1985). *J. Electrochem. Soc.*, 132, 814.
- [15] Alper, A. M. (1965). Zirconium dioxide and some of its binary systems. In: *High Temperatures Oxides*, Margrave, J. L. (Eds.), Academic Press: New York, pp. 117–166.
- [16] Toby, B. H. (2001). *J. Appl. Crystallogr.*, 34, 210.
- [17] Young, R. A. (1993). *The Rietvel Method*. Oxford University Press: New York.
- [18] Wachsman, E. D., Jiang, N., Frank, C. W., Mason, D. M., & Stevenson, D. A. (1990). *Appl. Phys. A: Mater. Sci. Process.*, 50, 545.
- [19] Arsenev, P. A., Bagdasarov, K. S., Niklas, A., & Ryazantsev, A. D. (1980). *Phys. Status Solidi A*, 62, 395.
- [20] Reisfeld, R., Saraidarov, T., Gaft, M., Pietraszkiewicz, M., Pietraszkiewicz, O., & Bianketti, S. (2003). *Opt. Mater.*, 24, 1.
- [21] Albella, J. M., Montero, I., & Martinezduart, J. M. (1987). *Electrochim. Acta*, 32, 255.
- [22] Leach, J. S. L. & Pearson, B. R. (1984). *Electrochim. Acta*, 29, 1263.
- [23] Leach, J. S. L. & Pearson, B. R. (1984). *Electrochim. Acta*, 29, 1271.
- [24] Silva, D. X. (2002). *Preparação e caracterização de ZrO₂ estabilizado a temperatura.*, UFSCar, São Carlos, PhD Thesis.
- [25] Bello, M. E. R. B. (2007). *Estudo do mecanismo da dopagem anódica em filmes de ZrO₂ crescidos eletroquimicamente*, UFSCar, São Carlos, PhD Thesis.